A NOVEL MODEL TO EVALUATE THE FATIGUE RESISTANCE OF NITI INSTRUMENTS: ROTATIONAL AND AXIAL MOVEMENT AT BODY TEMPERATURE

by

EVAN BAIRD

DDS, Dalhousie University, 2019

A THESIS SUBMITTED IN PARTIAL FULFILLMENT OF

THE REQUIREMENTS FOR THE DEGREE OF

MASTER OF SCIENCE

in

THE FACULTY OF GRADUATE AND POSTDOCTORAL STUDIES

(Craniofacial Science)

THE UNIVERSITY OF BRITISH COLUMBIA

(Vancouver)

June 2022

The following individuals certify that they have read, and recommend to the Faculty of Graduate and Postdoctoral Studies for acceptance, the thesis entitled:

A novel model to evaluate the fatigue resistance of NiTi instruments: Rotational and axial movement at body temperature.

submitted by Evan Baird in partial fulfillment of the requirements for

the degree of Master of Science

in Craniofacial Science

Examining Committee:

Dr. Ya Shen, Professor, Department of Oral Biological & Medical Sciences, UBC
Supervisor

Dr. Markus Haapasalo, Professor, Department of Oral Biological & Medical Sciences, UBC
Supervisory Committee Member

Dr. Ahmed Hieawy, Professor, Department of Oral Biological & Medical Sciences, UBC
Supervisory Committee Member

Dr. Fernanda Almeida, Professor, Department of Oral Biological & Medical Sciences, UBC
Additional Examiner

Abstract

Objective: The aim of the study was to develop a model of testing cyclic fatigue resistance of TruNatomy instruments of undergoing rotational and axial movement at body temperature, taking into consideration the size of the canal and location of the curvature.

Methods: Prime and Medium files were subjected to cyclic fatigue testing in simulated canals (at 37°C) using a model with either rotational movement only or rotational and axial movement simultaneously. Prime files were tested in 30/.04 and 30/.06 sized canals and Medium files were tested in 38/.04 and 40/.06 sized canals. The location of the curvature was unique for each canal, either in the apical, middle or coronal aspect of the canal.

Results: Files tested in the rotation and axial movement groups had a higher number of cycles to failure (NCF) compared to the rotation only group. Prime files had a higher NCF than Medium files. Files tested in apical curvatures had a higher NCF than files tested in middle and coronal curvatures.

Conclusion: Since rotational and axial movement of files led to greater fatigue resistance compared to rotational movement alone, future studies on fatigue resistance should implement a model with rotational and axial movement, as it is more comparable to a clinical scenario. Since Prime files had a higher NCF than Medium files, it is important to properly select the file for a particular canal. Apical curvatures led to greater fatigue resistance than curvatures in the coronal and middle third. Therefore, it is important that even when using a very flexible and fatigue resistant file, a proper glide path is developed and a suitable file size is selected when navigating these more coronal curvatures.

Lay Summary

The goal of this study was to establish a model for testing cyclic fatigue resistance of NiTi rotary files that provides a more accurate representation of a clinical scenario. Previous models have allowed files to rotate at working length until fracture, but in a clinical scenario the clinician is usually moving the file axially as it rotates. In this study TruNatomy files had fatigue resistance tested in an older model and a new model in which rotation and axial movement were used. Files tested in the new model using rotational and axial movement exhibited more fatigue resistance compared to files tested using rotation only. Since the new model is more representative of a clinical scenario and led to greater cyclic fatigue resistance, it makes sense to continue using a model that combines both rotational and axial movement so that clinicians can get a more accurate representation of the fatigue behavior.

Preface

This thesis is the principal work of Dr. Evan Baird, as per the requirements of a Master of Science in Craniofacial Science with a Diploma in Endodontics. The study was designed by Dr. Evan Baird and supervisor Dr. Ya Shen. The materials and models were developed by Dr. Evan Baird, Dr. N Dorin Ruse, Dr. Ya Shen and Dr. Ahmed Hieawy. The experimental testing was performed by Dr. Evan Baird. The results were statistically analyzed and interpreted with the assistance of Dr. Jolanta Aleksejuniene. Writing of the thesis was prepared by Dr. Evan Baird and edited by Dr. Ya Shen and Dr. Markus Haapasalo. Support and consultation were provided by Dr. Xiangya Huang, Dr. He Liu and Dr. Zhejun Wang.

Table of Contents

List of Figures

List of Abbreviations

A_s = Austenite transformation start temperature

A_f = Austenite transformation finish temperature

CM = controlled memory

DSC: Differential scanning calorimetry

ISO: International Organization for Standardization

M_s = Martensite transformation start temperature

M_f = Martensite transformation finish temperature

MFD = Maximum flute diameter

NCF: Number of cycles to failure

NiTi = Nickel titanium

rpm = revolutions per minute

SD: Standard deviation

Acknowledgements

I would like to thank my supervisor, Dr. Ya Shen, for her expertise, helpfulness and for creating a positive environment in which to complete this research. I would also like to thank Dr. N Dorin Ruse for allowing me to use his equipment and for helping me create this new model. I am thankful to Dr. Ahmed Hieawy for providing advice when setting up the materials and models. Furthermore, I would like to thank Dr. Markus Haapasalo for his support with the project. Additionally, I am grateful to Dr. Jolanta Aleksejuniene for her help with statistical analyses and interpretation, as well as Dr. Xiangya Huang, Dr. He Liu and Dr. Zhejun Wang for their help throughout the project.

I am thankful for my program director, Dr. Jeff Coil, as well as my clinical instructors for their mentorship throughout the program. I am also thankful for our CDAs, Shauna, Lois and Francisco, for their continued daily support in this program. To my co-residents, Dr. Ksenia Fedorova and Dr. Kiarash Shabehpour, thank you for being there for me every day since I began this program. To TKSC, thank you for pushing me in dental school to strive for excellence.

Dedication

I would like to dedicate this thesis to my parents, Hal and Lee-Ann Baird, and my sister, Haley Bergstrom, for supporting my pursuit of endodontics and helping me in any way they can so that I can achieve my goals. I would also like to dedicate it to Dr. Karmen Bleile, who taught me everything I know about the research process, which helped to open countless academic and professional opportunities for me. I would not be where I am today without her.

Chapter 1: Introduction

1.1 Purpose of endodontics

The underlying cause of pulpal and periradicular disease are microorganisms (Kakehashi et al., 1965; Sundqvist, 1976). Microorganisms can invade the root canal system in a variety of ways, such as through caries or defective restorations. Pulpal necrosis and, subsequently, apical periodontitis, occurs when there has been bacterial invasion of the root canal system. An inflammatory response is eventually initiated in the periapical region, causing deterioration of the periapical tissues (Bergenholtz, 1974). The goal of endodontic treatment is to eliminate microorganisms in the root canal system in order to prevent apical periodontitis or induce healing of apical periodontitis (Orstavik & Pitt Ford, 2008).

1.2 Elimination of microorganisms

To eliminate microorganisms from the root canal system, both mechanical and chemical processes are required. Mechanically, the canals can be debrided using hand and rotary files. However, this is not enough to eliminate the microorganisms from the canals, as walls of the canals can remain untouched and there may be ramifications throughout the root canal system that are not addressed (Siqueira et al., 1997). Therefore, chemical irrigation of the root canal system is also required, typically with sodium hypochlorite which has antimicrobial properties and the ability to dissolve tissue (Siqueira et al., 1997). Following disinfection of the root canal system, the system should be filled in order to prevent recontamination (Spangberg & Haapasalo, 2002). A restoration should then be placed to seal dentin and prevent bacteria from reentering the system (Ray & Trope, 1995).

1.3 Nickel-titanium instruments

Stainless steel files were traditionally used for instrumentation of the root canal system, until the introduction of nickel-titanium (NiTi) files (Walia et al., 1988). These NiTi files are composed of 56% nickel and 44% titanium by weight (Shen et al., 2013) and provide more flexibility and resistance to cyclic and torsional failure compared to stainless steel files (Walia et al., 1988). Advancements in metallurgy, surface treatment and file design have reduced the incidence of file fracture since rotary files were first introduced (Gambarini et al., 2008, Gutmann & Gao, 2012, Shen et al., 2013). Thermomechanical processing can be used to optimize the transformation behavior and microstructure of NiTi alloys, which has a positive influence on their mechanical properties (Gambarini et al., 2008, Bardsley et al., 2011, Gao et al., 2012 Shen et al., 2012). With respect to NiTi rotary files, there are currently five generations. The first generation consisted of files with radial lands (e.g., ProFile 0.04). These radial lands are flat surfaces between the flutes of the file and their purpose is to keep the file centered in the canal, at the expense of cutting efficiency (Haapasalo & Shen, 2013). The second generation (e.g., ProTaper) incorporated active cutting edges without radial lands, which increased cutting efficiency (Haapasalo & Shen, 2013). The third generation (e.g., ProFile Vortex) started to incorporate thermomechanical processing. The purpose of this was to influence the phase transformation temperatures of the NiTi so that the files would become more flexible (Shen & Haapasalo, 2013). M-Wire instruments (e.g., ProFile Vortex, Profile GT-X) were created by applying heat treatments to NiTi wire blanks. The fourth generation of files use reciprocating motion (e.g., WaveOne Gold), which rotate in the cutting direction and then disengage in the opposite direction (Yared, 2007). This may decrease the formation of intra-dentinal cracks and decrease risk of fatigue file fracture (De Deus et al., 2010). Whereas previous systems had a

sequence of files that had to be used to work up to a desired size, a single reciprocating file can be sufficient to instrument a canal (Yared, 2007). Fifth generation files (e.g., ProTaper Next) include files designed so that the center of mass and center of rotation are offset (Haapasalo & Shen, 2013). This minimizes the contact surface area between the dentin and file, which lessens the taper lock and torque (Haapasalo & Shen, 2013).

1.3.1 Physical properties of NiTi instruments

Structurally, NiTi can exist in three states (austenite, martensite, R-phase). NiTi has both superelasticity and shape memory. When stress is applied to a superelastic metal, up to 8% strain may be recovered (Shen et al., 2013). This is due to martensite transformation, which is stress induced. Stresses lead to a transformation of austenitic crystalline structure into martensitic crystalline structure, which can withstand an increase in stress, without leading to more strain (Shen et al., 2013). Therefore, the metal has the ability to return to its original shape after deformation. Shape memory is the ability of the material to return to its original shape after heat application (Otsuka & Ren, 2005). At higher temperatures the austenitic phase is present, which makes the file stronger and stiffer compared to the martensitic phase (Shen et al., 2013). The martensitic phase is present at lower temperatures and is softer and more flexible (Shen et al., 2013). When the temperature of martensitic NiTi is increased, it changes to austenite. The temperature at the starting point of this process is the austenite transformation start temperature (A_s). The temperature at the completion of this process is the austenite transformation finish temperature (A_f) (Shen et al., 2013). Above the A_f, the shape memory transformation is complete and will display its superelastic properties. By contrast, when the temperature of austenitic material is decreased, it begins to transform into martensite. The temperature at the starting point

of this process is the martensite transformation start temperature (M_s). The temperature at the completion of this process is the martensite transformation finish temperature (M_f). The A_f for most conventional NiTi files is at or below room temperature, while for newer controlled memory (CM) files (e.g., TYP) it is above body temperature. Therefore, conventional files are typically in the austenite phase when used clinically, compared to CM files which are typically in the martensitic phase (Shen et al., 2013). The transformation of austenite to martensite or vice versa can occur in one or two stages. The involvement of two stages includes the formation of an intermediate R-phase (Otsuka & Ren, 2005). This phase can be temperature or stress-induced and exhibits shape memory and superelasticity (Santos et al., 2016). This phase has a low Young's modulus of elasticity, making it more flexible than martensite (Santos et al., 2016). Earlier generations of NiTi instruments were in the austenitic phase at body and room temperature, making them more stiff and less resistant to fatigue (Brantley et al., 2002). By heat treating the files, a more flexible and fatigue resistant file is created because at body temperature the file will exist in a more martensitic phase (Otsuka & Ren, 2005).

1.3.2 Cyclic and torsional fatigue

There are two fatigue processes that can lead to NiTi rotary file fracture, cyclic fatigue and torsional fatigue. Cyclic fatigue occurs when an instrument is rotating freely in a curvature and is generating tension/compression cycles at the point of maximum flexure (Pruett et al., 2007). Cyclic fatigue resistance decreases with extended use of the file (Tewari et al., 2017). The fracture will occur at the canal's point of maximum curvature (Pruett et al., 2007). The risk of cyclic fatigue failure depends on the morphology of the root canal and the fatigue resistance of the file. The components of the morphology that will increase the likelihood of cyclic fatigue

failure are large angle of curvature, small radius of curvature and a long arc length of the curvature (Pruett et al., 1997). Curvatures located more coronally in the canal are at a higher risk of leading to cyclic fatigue failure (Alghamdi et al., 2020, Sobotkiewicz et al., 2021). Files with larger diameter and taper will have decreased cyclic fatigue resistance (Pruett et al., 1997). The first step in the process by which this cyclic fatigue failure occurs includes crack initiation, which originates near the cutting edge of the file or defects on the files surface (Cheung et al., 2007). The second step is crack propagation, which microscopically is seen as striations that start on the periphery of the file and move toward the centre (Cheung et al., 2007). The third step, final (fast) fracture, is seen microscopically as dimples in the centre of the fractured surface (Cheung et al., 2007). Torsional fatigue occurs when an instrument tip gets locked and the shank continues to rotate (Cheung et al., 2007; Kitchens et al., 2007). The shear strength of the NiTi can be exceeded, which will result in fracture (Cheung, 2009). In torsional fatigue failure, the fatigue striations seen in cyclic fatigue failure are not present (Cheung et al., 2007). The consequence of fracturing an instrument is that it may not be possible to remove or bypass it, potentially leaving a significant amount of microorganisms in the canal depending on how much cleaning and shaping was performed prior to the fracture. However, it has been shown that the success rate of root canal treatments with or without a fractured instrument present does not typically impact the success of the treatment (Crump & Natkin, 1970; Panitvisai et al., 2010). However, this is dependent on the level of disinfection of the canal prior to instrument separation. Therefore, it is desirable to avoid fracturing a file to ensure that the root canal system is adequately disinfected.

1.3.3 Methods of testing cyclic fatigue resistance

There currently is no standardized method to test cyclic fatigue resistance of NiTi rotary files. Previous methods of testing cyclic fatigue resistance include curved metal tubed, sloped and grooved metal blocks, three-point bending apparatuses and simulated canals (Plotino et al., 2009). The most common modern technique is to use simulated canals, allowing files to be positioned at working length and allowed to rotate until fracture. This is typically done at room temperature. Cyclic fatigue resistance can also be influenced by the way in which the file is being used. In most modern models of cyclic fatigue resistance testing, the instrument rotates, but does not move axially. Therefore, alternative compressive and tensile stresses are concentrated in one area of the instrument, which induces microstructural changes in the alloy (Lopes et al., 2013). In a model with rotational and axial movement, the instrument moves axially along the curvature, which allows stresses to distribute along the shaft of the instrument (Lopes et al., 2013). By preventing stress concentration in the same area, the fatigue life of the instrument could be extended. There have been a limited number of studies which have included axial movement in addition to rotation to measure cyclic fatigue (De-Deus et al., 2014; Keskin et al., 2018; Li et al., 2002; Lopes et al., 2013, Ozyurek et al., 2016; Ray et al., 2007; Topcuoglu et al., 2017) and there are no definitive guidelines as to how this should be done. The device used to create axial movement also varies between the studies that have included it, and none of them have included testing at body temperature as part of the model. A recent study showed that at lower temperatures, these files exhibit greater cyclic fatigue resistance (Shen et al., 2018). If files are being tested at room temperature, for example, the results may not be representative of when the files are used on an actual patient. The most common amplitude for axial movement used is 3 mm (De-Deus et al., 2014; Keskin et al., 2018; Lopes et al., 2018) and the most common cross-

head speed is 1 mm/s (Li et al., 2002). A dynamic model was recently used to investigate the mechanical properties of TruNatomy (Dentsply Sirona, Ballaigues, Switzerland) files, including both rotational and axial movements simultaneously (Peters et al., 2020). However, only torque and force were measured and the files were not programmed to rotate and move axially until fracture. It is of interest to develop a model that allows for files to be programmed to undergo rotational and axial movement at body temperature until fracture, as this is more representative of a clinical scenario than a model with rotational movement only.

1.3.4 Differential scanning calorimetry (DSC)

A DSC test is used to determine the temperatures at which NiTi will begin and finish its phase transformations (Shen & Cheung, 2013). When transitioning from austenite to martensite, an exothermic reaction occurs, whereas from martensite to austenite an endothermic reaction occurs. In a DSC test an experimental instrument and control are heated and cooled at the same rate. When the phase of the instrument is transformed, DSC can measure small differences in enthalpy between the instrument and control. Knowing this information makes it more predictable what type of behavior the file will exhibit clinically at body temperature.

1.3.5 TruNatomy

A new NiTi rotary file system, TruNatomy, has recently been introduced to the market. This system is designed to instrument root canal systems to a continuously tapering preparation with a goal of preservation of peri-cervical dentin (Van der Vyver et al., 2019). The manufacturers of this file claim that this system offers more simplicity, safety, cutting efficiency

and mechanical properties compared to previous generations of endodontic rotary instruments (Van der Vyver et al., 2019).

The maximum flute diameter (MFD) of these instruments is 0.8 mm, which is smaller than many conventional rotary instruments, many of which have an MFD of ~1.1 mm (Van der Vyver et al., 2019). The thermal treatments for this system have been refined to create a flexible file system (Van der Vyver et al., 2019).The instruments have approximately the same apical sizing as the most commonly used NiTi rotary instruments, but they have a regressive taper as the instrument progresses coronally to allow each instrument to have an MFD of 0.8 mm (Van der Vyver et al., 2019). The goal of this is to preserve peri-cervical dentin that is often compromised with other rotary filing systems. The TruNatomy system consists of an Orifice Modifier, a Glider and three shaping files (Small, Prime, Medium) for different clinical applications (Van der Vyver et al., 2019). All TruNatomy instruments are designed to run in a continuous, 360° motion at 500 rpm, with a torque setting of 1.5 Ncm.

The Prime instrument is the main shaping instrument and the manufacturers recommend that it be used in the majority of cases (Van der Vyver et al., 2019). It has a tip size of ISO 26 and decreasing taper averaging to be 0.04. The Medium file is used for larger canals and when more apical shaping is required. It has a tip size of ISO 36 and a decreasing taper of approximately 0.03. There is also the Small shaping file, which is used for extensively curved canals where the Prime file is not able to reach working length easily. It has a tip size of ISO 20 and a taper averaging to be 0.04.

1.4 Rationale

In most modern models of cyclic fatigue resistance testing, the instrument rotates, but does not move axially. The alternative compressive and tensile stresses are concentrated in one area of the instrument, creating a scenario that is not comparable with clinic practice. In a model with rotational and axial movement, the instrument moves axially along the curvature, which allows stresses to distribute along the shaft of the instrument. By preventing stress concentration in the same area, the fatigue life of the instrument could be extended. This is more representative of a clinical scenario and therefore may be a more appropriate model for fatigue testing going forward. There have been a limited number of studies which have included axial movement in addition to rotation to measure cyclic fatigue and there are no definitive guidelines as to how this should be done. The device used to create axial movement also varies between the studies that have included it, and none of them have included testing at body temperature as part of the model. By creating a model which tests files with both rotational and axial movement at body temperature, it may provide a result that is more comparable to a clinical scenario and will provide clinicians with a better idea of the fatigue resistance of a particular file when they are deciding which files to use.

1.5 Aims

- To develop a model of testing cyclic fatigue resistance at body temperature of rotary NiTi instruments by comparing cyclic fatigue resistance of TruNatomy instruments undergoing rotational and axial movement, or rotational movement only, taking into consideration the size of the canal and location of the curvature
- To examine the phase transformation temperatures of TruNatomy instruments

1.6 Null hypotheses

- There will be no difference in fatigue resistance of TruNatomy instruments between rotational and axial movement and only rotational movement at body temperature
- The location of canal curvature does not affect the fatigue resistance of TruNatomy files
- The size of the canal does not play a role in the fatigue resistance of NiTi files
- Different sizes of TruNatomy files have the same fatigue life.

Chapter 2: Materials and Methods

2.1 Sample size calculation

The sample size was calculated using G*Power test version 3.1.94 software (Heinrich-Heine-Universitat Dusseldorf, Brunsbuttel, Germany). The significance value was set at .05, and the power at 80. The software calculated 10 files per group. 12 files per group were included in the study. The total sample size was 288 files (144 Prime, 144 Medium).

2.2 Rotational cyclic fatigue test

Prime (26/.04v) and Medium (36/.03v) TruNatomy (Dentsply Sirona, Ballaigues, Switzerland) files were subjected to cyclic fatigue testing. The simulated ceramic canals were milled using an InCoris ZI zirconium oxide disc (Dentsply Sirona, Bensheim, Germany) and the inLab MC X5 digital computer-aided design and computer-aided manufacturing system (Dentsply Sirona). For the Prime files, the size of one set of simulated canals was 30/.04 and another set was 30/.06. For the Medium files, the size of one set of simulated canals was 38/.04 and another set was 40/.06. Each curvature had an angle of 60° and a radius of curvature of 3 mm. The total length of each canal was 16 mm and the arc length was 3.14 mm. Each file was subjected to three different types of curvatures. The distance between the canal orifice and the location of the curvature (DOC) was 5, 8, and 11 mm, representing coronal, middle and apical curvatures, respectively (Figure 1).

Polyvinyl siloxane impression material was used to create a custom jig to stabilize the simulated canals. The jig and simulated canals were placed in a transparent glass container filled with deionized water (Figure 2A-F). A piece of transparent fiber glass was placed over the

simulated canals to ensure that the files remained within the confines of the canal during fatigue testing. Plastic plumber screws were used to stabilize the jig and simulated canal block against the glass container (Figure 2B). The glass container was stabilized using Velcro on a flat piece of wood. This assembly was then placed on a flat metal surface. A small container water heater was used to heat the water to 37°C and then a temperature sensor maintained the temperature at 37°C +/- 1°C (Figure 2C). The files were tested using an 8:1 reduction handpiece connected to a ProMark Endo motor (Dentsply Sirona). Twelve files for each group were tested (12 groups total). The files were placed 1 mm short of working length and rotated at 500 rpm and 1.5 Ncm torque (as per manufacturer recommendation) until fracture. The number of cycles to fracture (NCF) was calculated by dividing the time to fracture by 60 and multiplying by the number of revolutions per minute. The length of each fractured fragment was collected, and its length was measured under a surgical operating microscope.

2.3 Rotational and axial cyclic fatigue test

Another 12 groups (n = 12) were subjected to a combination of both rotational and axial cyclic fatigue testing, using the same simulated canals and types of curvatures as in the groups testing rotational movement only. However, in these groups the handpiece was attached to an Instron machine (Instron corp., Canton, MA) using an acrylic jig and a load cell was attached to the metal plate holding the glass container assembly, in order to measure the force exerted during axial movement. The files were placed 4 mm from working length and the Instron machine was programmed to move the files axially in 3 mm amplitudes at 1 mm/s (Figure 2D-F). The files were allowed to rotate at 500 rpm and 1.5 Ncm torque, as well as move axially until fracture.

The NCF and force (N) were recorded, and the length of each fractured fragment was collected and measured under a surgical operating microscope (Global, St Louis, MO).

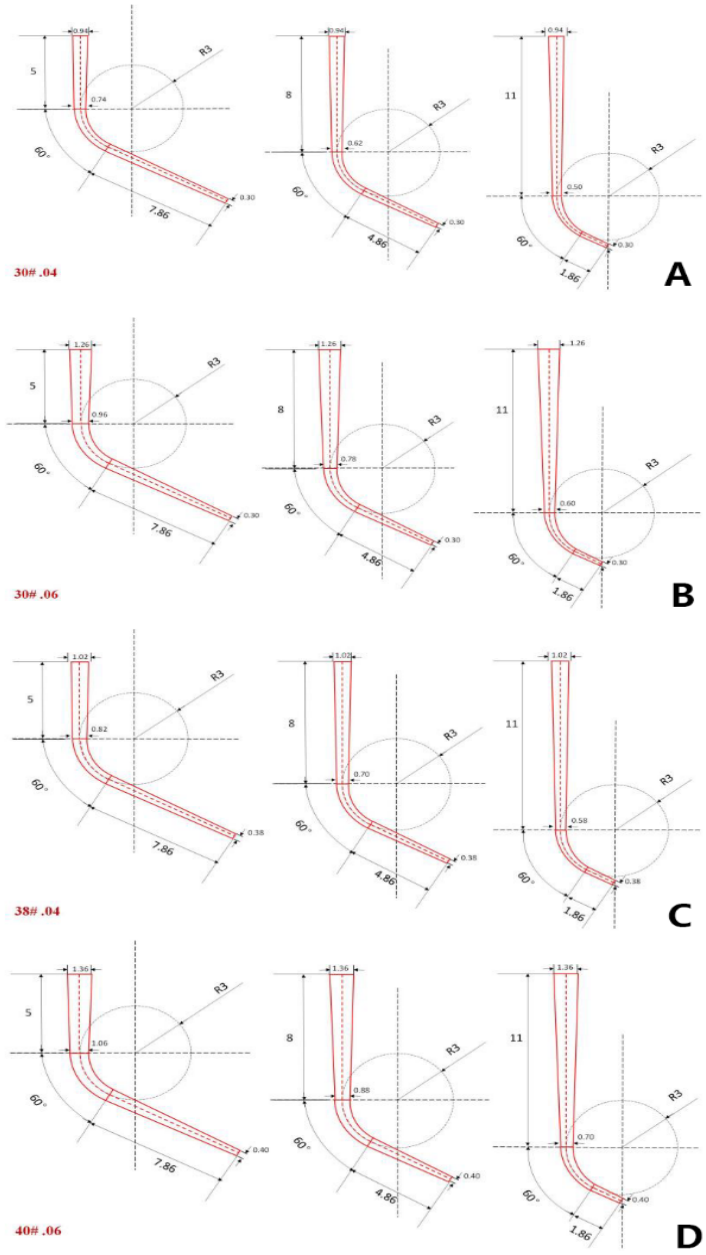

Figure 1. (A-D) Schematic diagrams of 3 curvature locations of the canals (5mm, 8mm, 11mm). Prime files were tested using (A) 30/.04 and (B) 30/.06 tapered canals. Medium files were testing using (C) 38/.04 and (D) 40/.06 tapered canals.

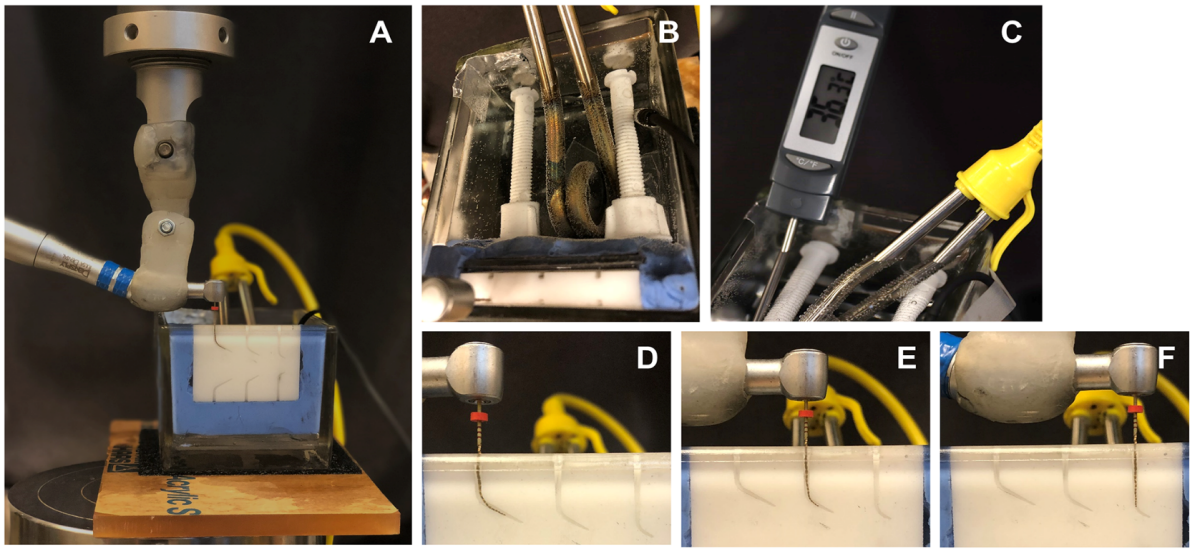

Figure 2. (A-F) The setup of the fatigue test. (A) The handpiece was attached to the Instron machine with the file placed 4mm short of working length for the rotational and axial movement conditions. (B) Plumber screws were used to secure the zirconium block against the glass container. (C) A small container heat source and a temperature sensor were used to heat the water and control the temperature. A thermometer was used to ensure the temperature sensor was calibrated properly. (D-F) The arrangement of the artificial canals.

2.4 Differential scanning calorimetry

Eight new medium TruNatomy files were subjected to DSC testing. These files were separated into apical (D0-D4) and coronal (D7-D11) segments using a diamond bur with water coolant. The DSC2500 machine (TA Instruments, New Castle, USA) was used to investigate the thermal behavior of these segments. Each fragment was weighed with an electronic balance and placed in a pre-weighed aluminum cell consisting of a Tzero pan and a Tzero Hermetic Lid (TA Instruments, New Castle, USA). The reference sample was an empty Tzero pan sealed with a Tzero Hermetic Lid. The sample was cooled to -75°C using liquid nitrogen. Then it was heated

at 10°C/min until it reached 100°C. The sample was then cooled to -75°C at 10°C/min. The data was analyzed using TRIOS Software (TA Instruments, New Castle, USA), which was used to analyze the thermal behavior of each sample. The phase transformation temperatures (A_s, A_f) were determined from thermograms using the TRIOS software function Onset Point.

2.5 Statistical analysis

Statistical analysis was performed using SPSS software (SPSS for Mac Version 26.0; IBM Corp, Armonk, NY). Normality was tested using the Kolmogorov-Smirnov test. The assumption of homogeneity of variance was tested using Levene's test. Independent samples t-tests were used to compare differences in NCF between rotational movement only and rotational + axial movement groups, and prime and medium file groups. One-way analysis of variance was used to compare the average NCF between the different curvatures, as well as between the different sizes of canal. Post-hoc comparisons were made using Bonferroni tests. Multiple linear regression was used to examine the relationship between NCF and model type, file type, curvature location and canal size.

Chapter 3: Results

Section 3.1 Rotation only vs. rotation + axial groups

The NCF of rotation only and rotation + axial groups is displayed in Figure 3. Files tested in the rotation + axial groups had a significantly higher NCF compared to the rotation only groups ($p < .001$). The length of the fractured fragment is displayed in Figure 4. Files tested in the rotation + axial groups had a significantly lower length of fractured fragment compared to files tested in the rotation only group ($p < .05$)

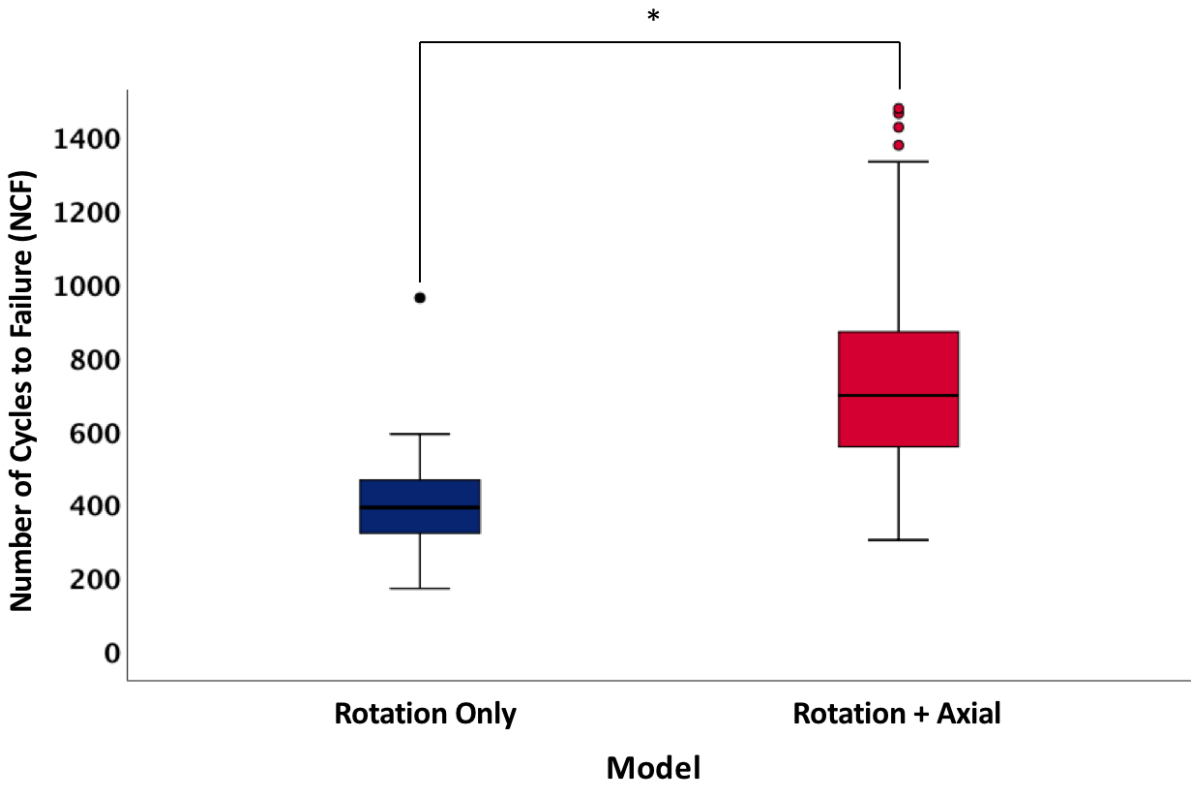

Figure 3. The NCF (mean +/- standard deviation) of TruNatomy files undergoing rotation only and rotation with axial movement. An asterisk indicates a significant difference between groups ($p < .001$).

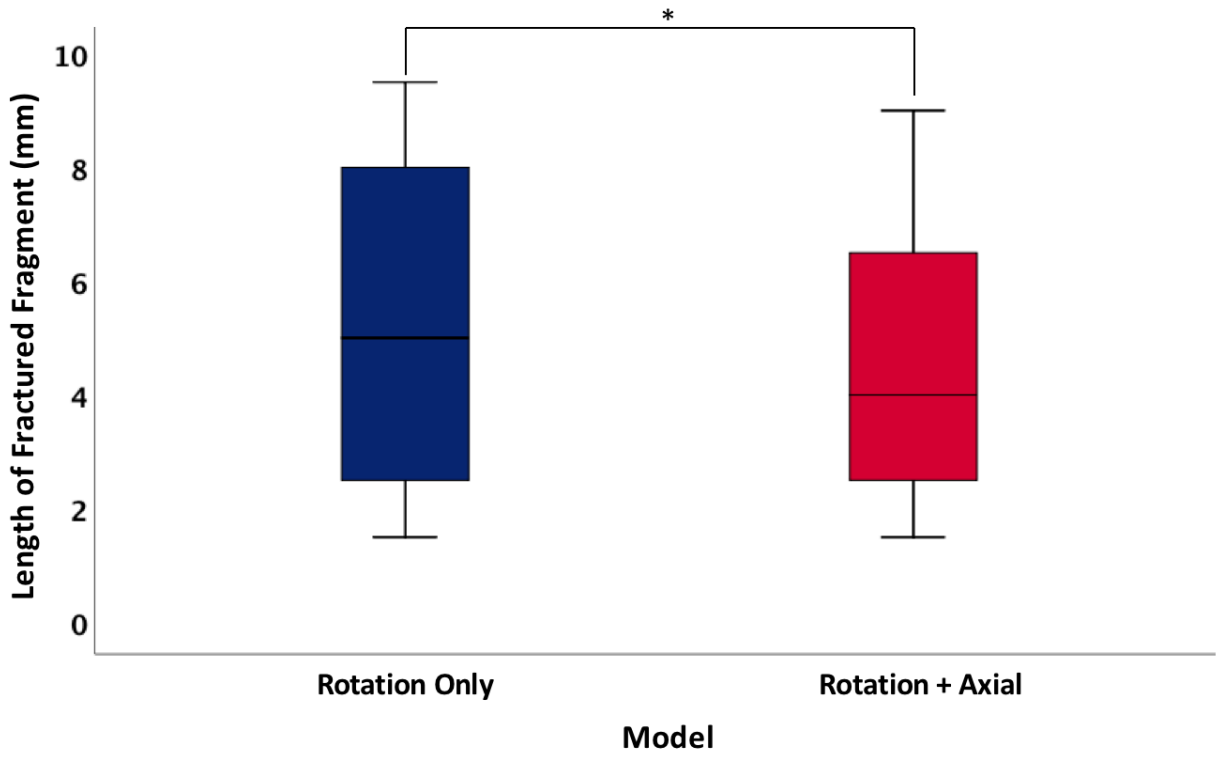

Figure 4. The length of fractured file fragments between the rotation only group and rotation + axial group. An asterisk indicates a significant difference between groups ($p < .05$).

Section 3.2 Prime vs. medium files

Prime files had a significantly higher NCF compared to Medium files ($p < .05$) (Figure 5). There was no significant difference in the length of the fractured fragments between Prime and Medium files ($p > .05$) (Figure 6).

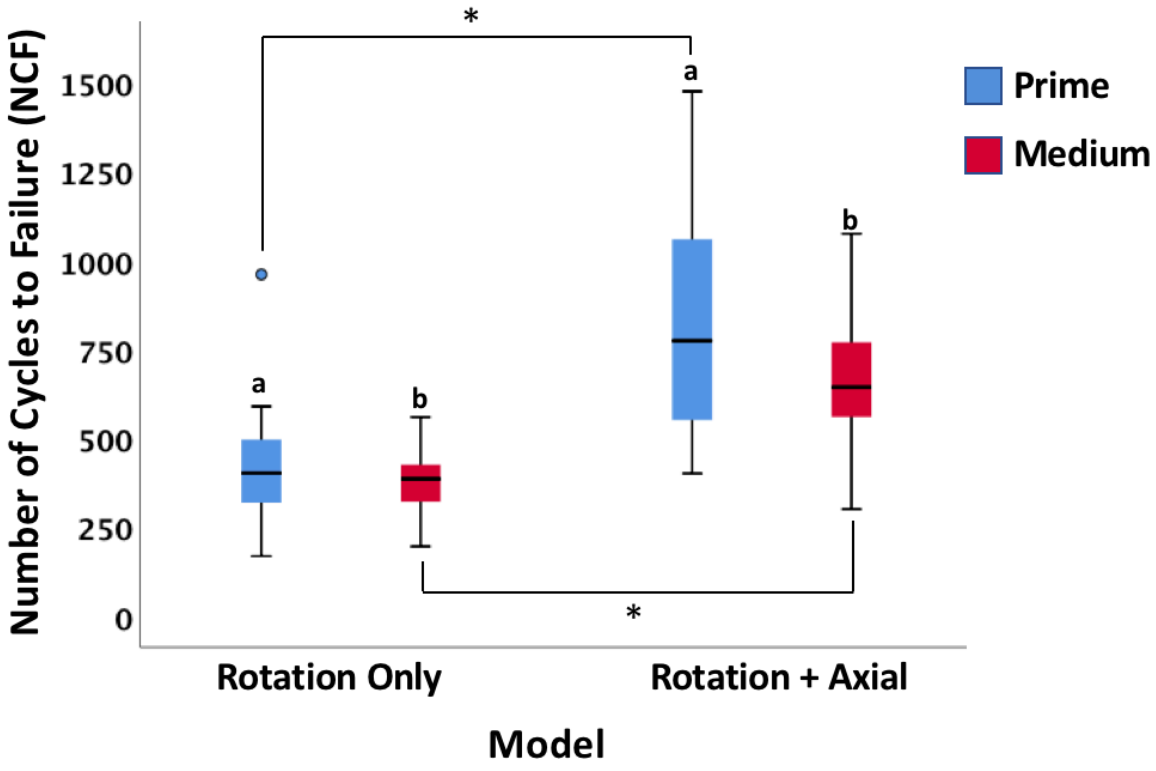

Figure 5. The NCF of Prime and Medium TruNatomy files undergoing rotation only and rotation with axial movement. Different lowercase letters indicate a significant difference within groups ($p < .05$). An asterisk indicates a significant difference for each file between groups ($p < .05$).

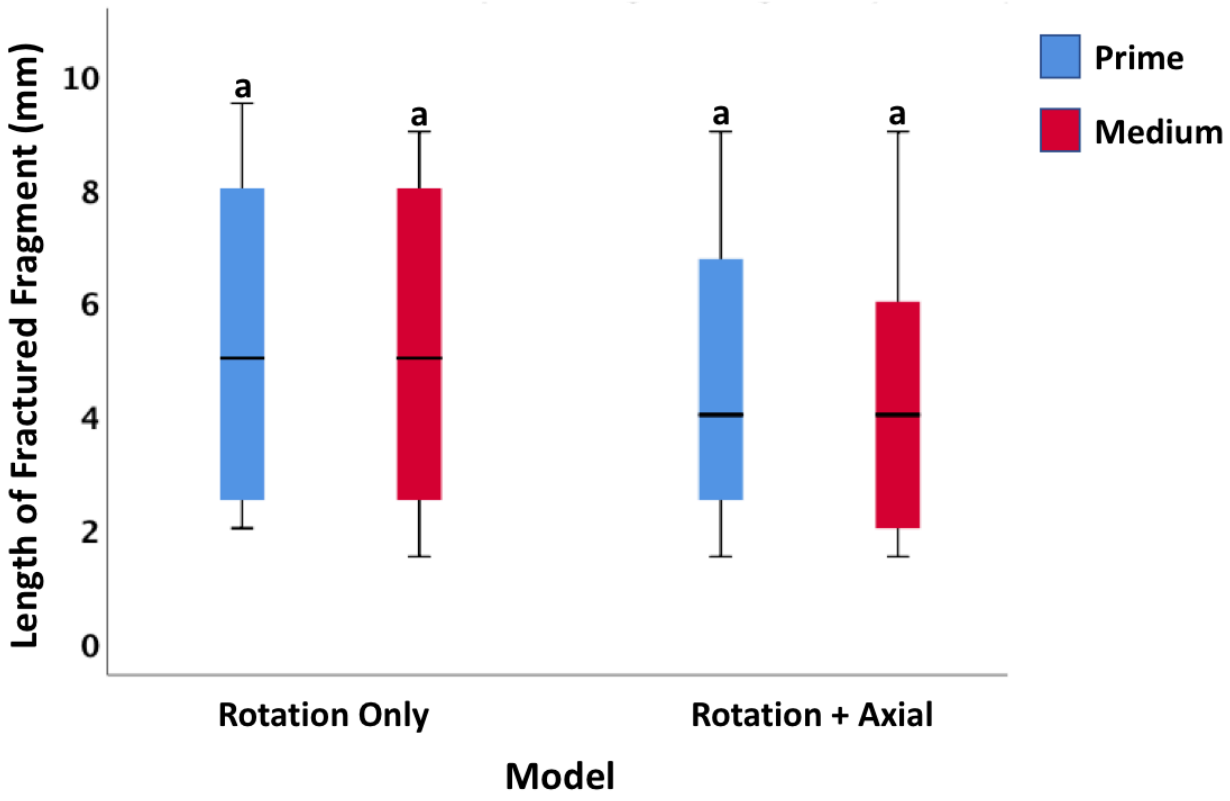

Figure 6. The length of fractured file fragments between Prime and Medium files, within the rotation only group and rotation + axial group. Different lowercase letters indicate a significant difference within groups.

Section 3.3 Curvature comparisons

The NCF of apical, middle and coronal curvatures for each model is displayed in Figure 7. Apical curvatures led to higher NCF compared to middle ($p < .05$) and coronal ($p < .001$) curvatures. Middle curvatures led to higher NCF compared to coronal ($p < .001$). The length of fractured fragments of apical middle and coronal curvatures for each model is displayed in Figure 8. Apical curvatures had the smallest fragments, followed by middle and coronal curvatures ($p < .05$).

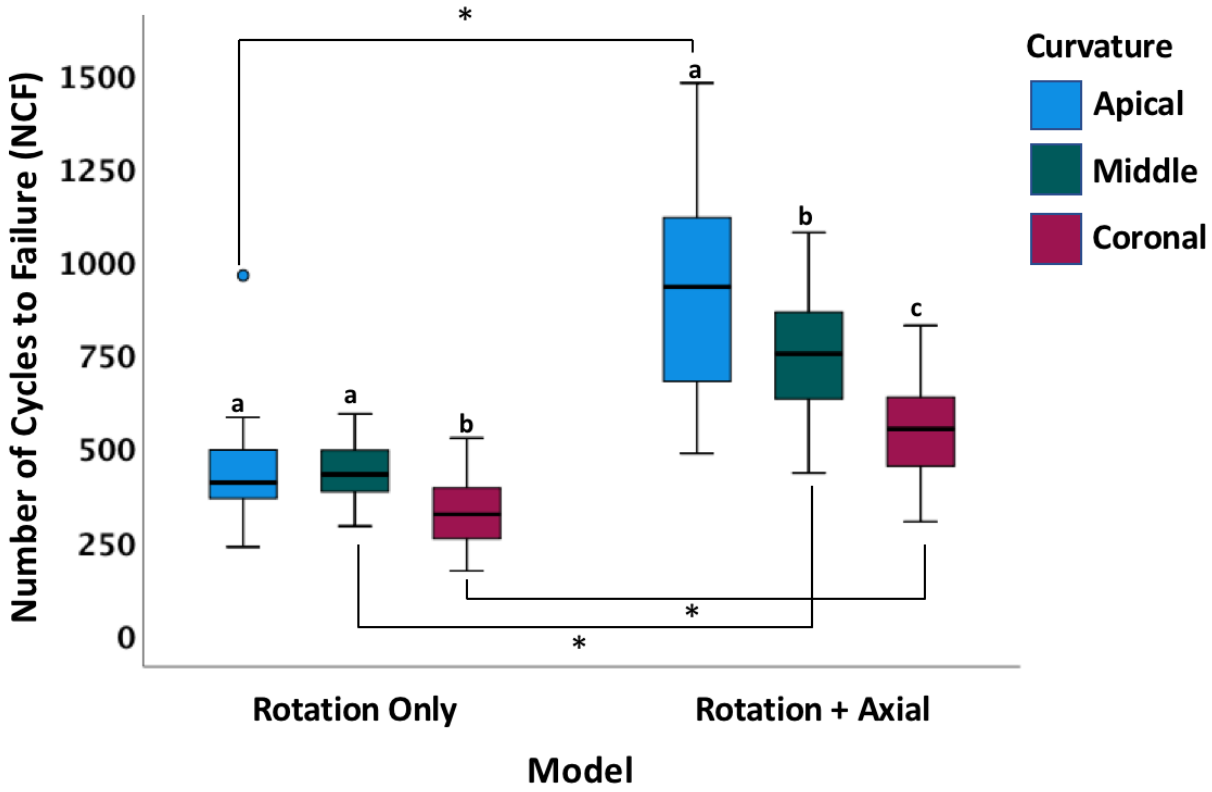

Figure 7. The NCF for files used in apical, middle and coronal curvatures undergoing rotation only and rotation with axial movement. Different lowercase letters indicate a significant difference within groups ($p < .05$). An asterisk indicates a significant difference between groups ($p < .05$).

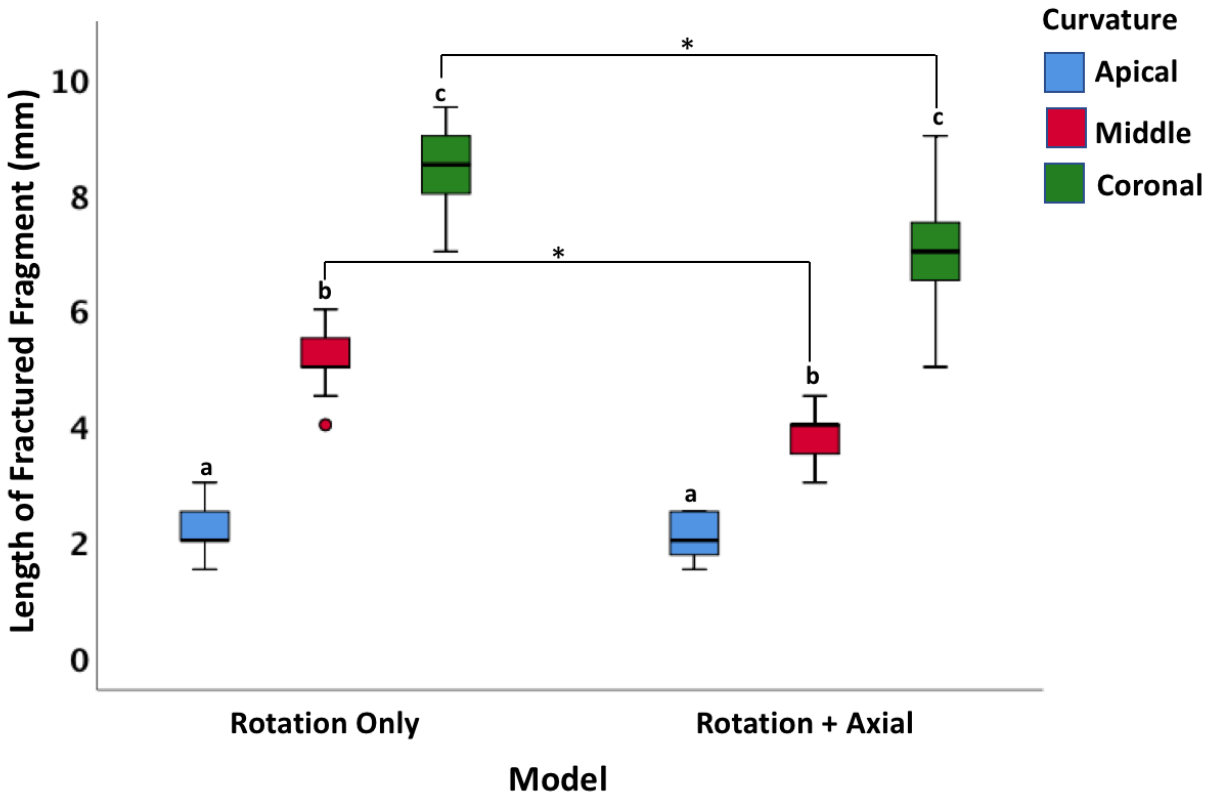

Figure 8. Length of fractured fragments for files used in apical, middle and coronal curvatures undergoing rotation only and rotation with axial movement. Different lowercase letters indicate a significant difference within groups ($p < .05$). An asterisk indicates a significant difference between groups ($p < .05$).

Section 3.4 Canal taper comparisons

There was no difference in NCF for the taper of the simulated canals between 30/.04 and 30/.06 for Prime files and also between 38/.04 and 40/.06 for Medium files within both rotation only and rotation + axial groups ($p > .05$) (Figure 9). The length of the fractured fragments did not differ between the different canal tapers within both rotation only and rotation + axial groups ($p > .05$)

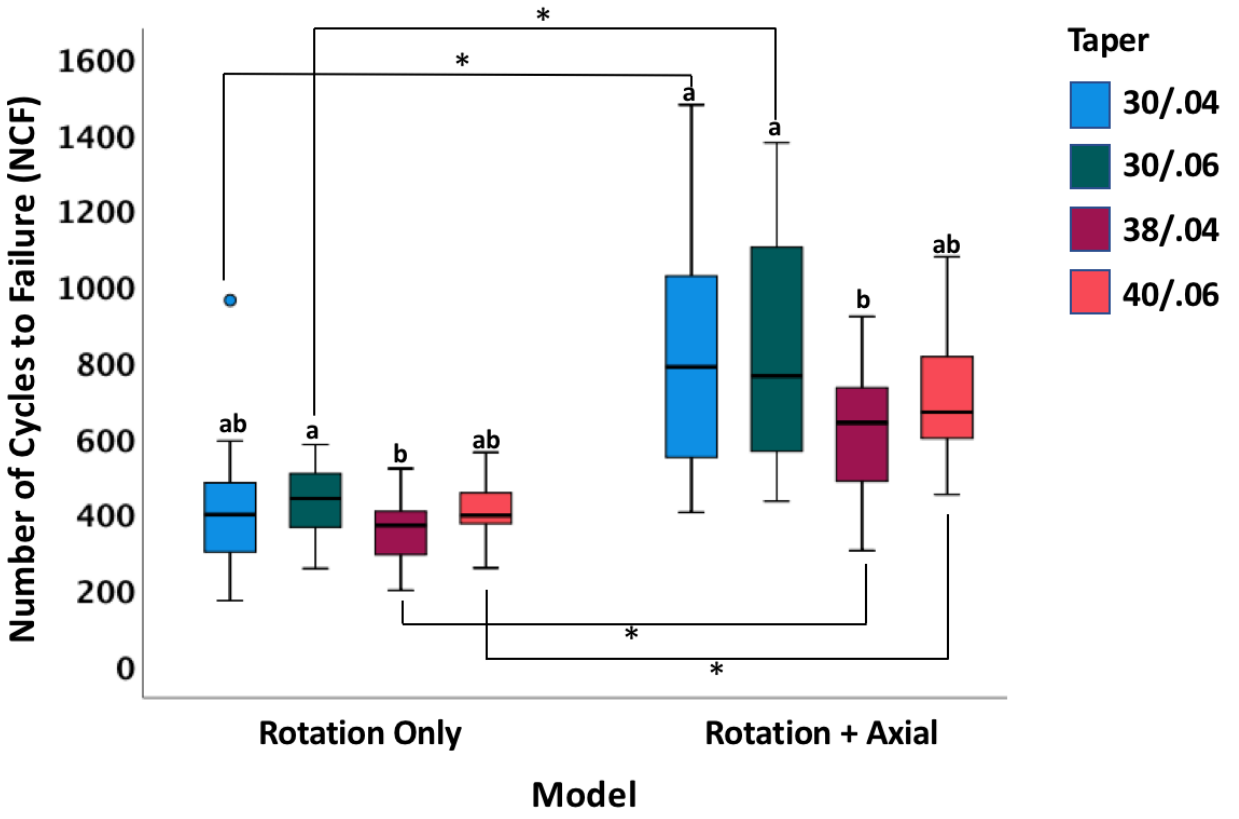

Figure 9. The NCF for files used in canals with size 30/.04, 30/.06, 38/.04 and 40/.06 undergoing rotation only and rotation with axial movement. Different lowercase letters indicate a significant difference within groups ($p < .05$). An asterisk indicates a significant difference between groups ($p < .05$).

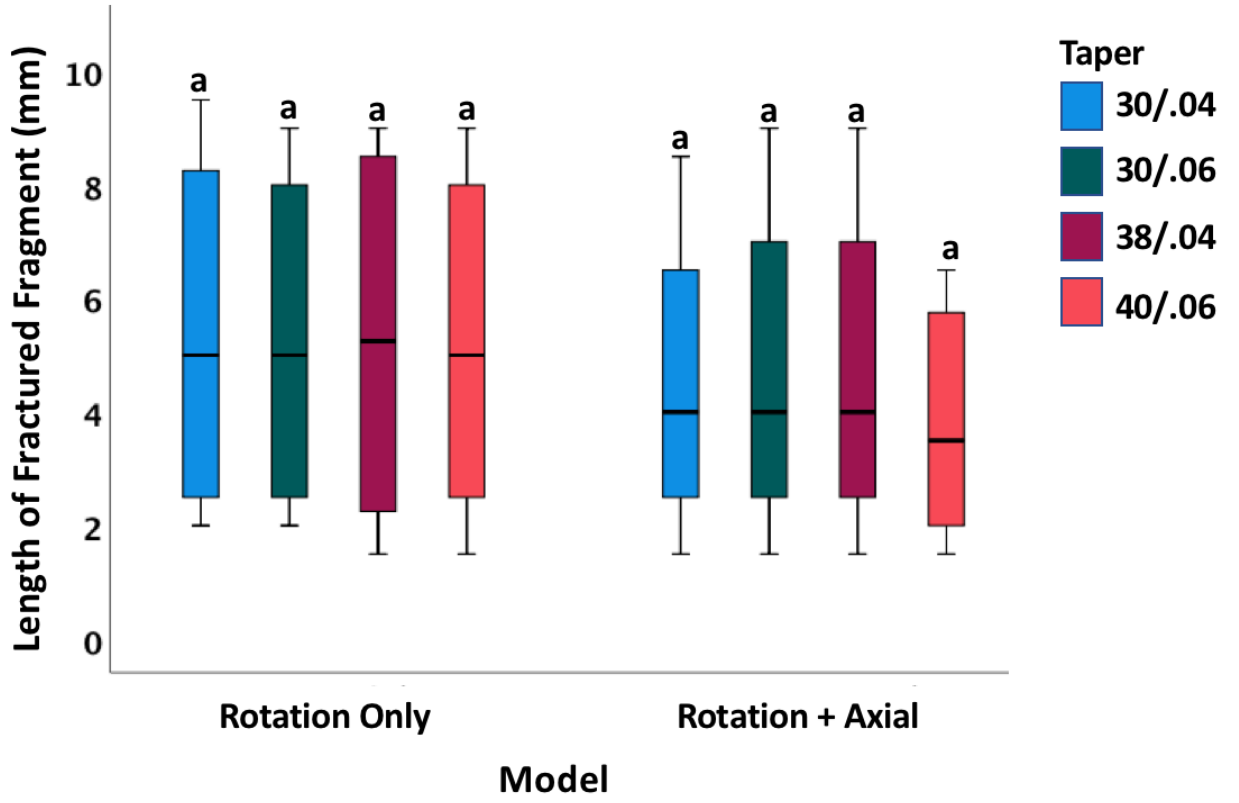

Figure 10. The length of fractured fragments for files used in canals with size 30/.04, 30/.06, 38/.04 and 40/.06 undergoing rotation only and rotation with axial movement. Different lowercase letters indicate a significant difference within groups.

Section 3.5 Regression analysis

Multiple linear regression revealed that 63.6% of the variation in NCF is explained by the predictors (model, file, curvature, taper). The overall linear regression model was significant ($p < .001$). Model type (type of movement) had the greatest influence on NCF ($\beta_1 = .663$, $p < .001$), indicating that NCF tends to be higher with rotation combined with axial movement compared to rotation alone. Curvature in the middle third tended to lead to higher NCF compared to coronal third ($\beta_1 = .283$, $p < .001$). Curvature in the apical third tended to lead to higher NCF compared

to coronal third ($\beta_1 = .445$, $p < .001$). There was no difference in the influence on NCF between the canals of size 30/.04 and 30/.06 ($\beta_1 = .036$, $p > .05$). The canal size of 38/.04 led to lower NCF compared to size 30/.04 ($\beta_1 = -.219$, $p < .001$). The size of canal 40/.06 led to lower NCF compared to 30/.04 ($\beta_1 = -.087$, $P < .05$). There was no influence of file type when all other predictors were included in the analysis.

Section 3.6 Differential scanning calorimetry

The DSC curves for heating and cooling of new and fractured Medium TruNatomy files are presented in Figures 11 and 12. The thermal behaviour is similar in both DSC plots. The A_f temperatures for the apical and coronal segments were 30.32°C and 30.88°C.

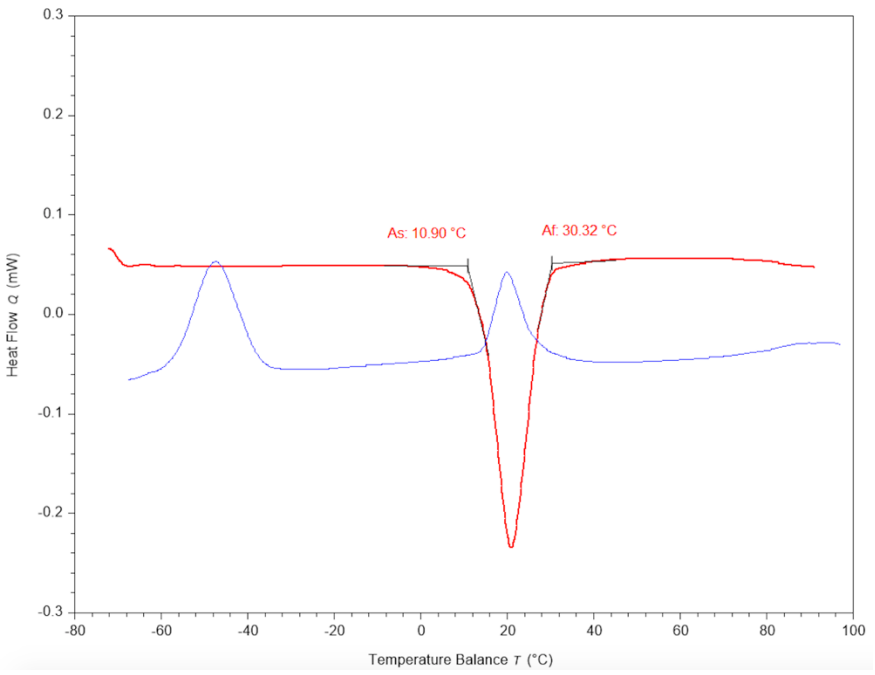

Figure 11. DSC curve for apical Medium TruNatomy fragments

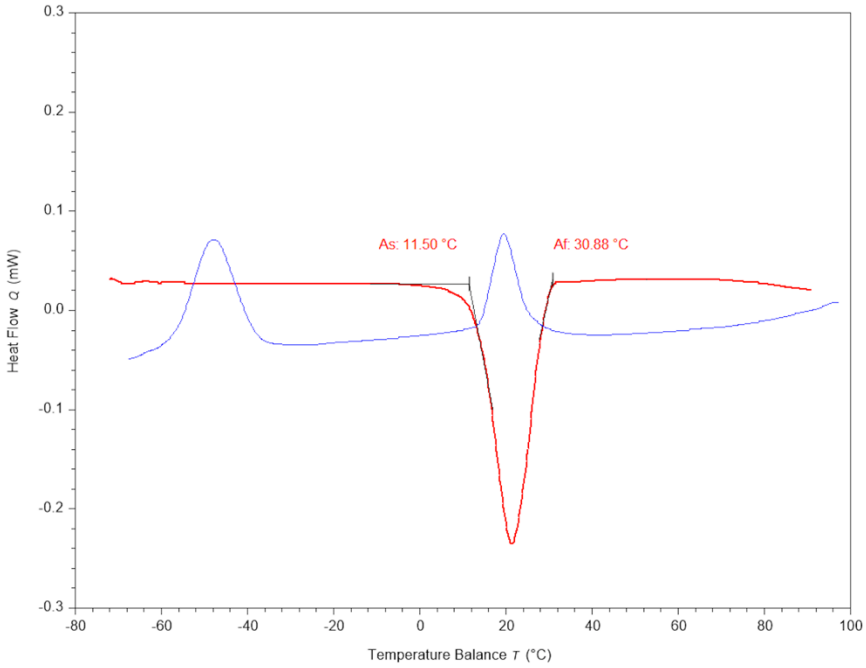

Figure 12. DSC curve for coronal Medium TruNatomy fragments

Chapter 4: Discussion

In the majority of cyclic fatigue resistance studies, the instruments are allowed to rotate, but do not move axially. Given that axial movement is essential when instrumenting a root canal, it would be of benefit for a standardized model to be developed for future cyclic fatigue studies. In the current study, a model was developed in which files were programmed to undergo both rotational and axial movement at body temperature, and this model was compared to a model where the file was programmed to rotate only. Overall, it was found that files tested in the rotation with axial movement groups had a greater NCF than those tested in the rotation only groups. An explanation for this is that in the rotation only groups, compressive and tensile stresses were concentrated in one area of the file, whereas for files that underwent rotation and axial movement, the files move axially along the curvature, which allows stresses to distribute along the shaft of the instrument (Lopes et al., 2013). By allowing forces to distribute along the shaft, the fatigue life of the instrument could be extended (Lopes et al., 2013). There have been a limited number of studies which have included axial movement in addition to rotation to measure cyclic fatigue at room temperature (De-Deus et al., 2014; Keskin et al., 2018; Li et al., 2002; Lopes et al., 2013, Ozyurek et al., 2016; Ray et al., 2007; Topcuoglu et al., 2017). Since the limited number of studies that have tested axial movement all tested the files at room temperature, this does not accurately represent a clinical scenario at body temperature. Body temperature should therefore be implemented in any model testing cyclic fatigue resistance. Given the stark contrast between the fatigue resistance of TruNatomy files tested in rotation only and rotation and axial conditions, it would seem to be of benefit for future studies to use a method in which the files are able to rotate and move axially simultaneously at body

temperature. This would be more representative of a clinical scenario and give clinicians a better idea of the number of cycles that a particular file could be used before fracturing.

Another factor considered in this study was the location of curvature. Overall, apical curvatures led to higher NCF compared to middle and coronal curvatures, and middle curvatures led to higher NCF compared to coronal. These findings are consistent with previous studies that examined the influence on curvature location on fracture resistance with continuous (Alghamdi et al., 2020) and reciprocating (Sobotkiewicz et al., 2021) file systems. They found that files had low fatigue resistance when the curvature was located in the coronal and middle thirds compared to the apical third. This is important, as it indicates that even though new technology has allowed the creation of very flexible file systems, these files are still more prone to fracturing when used in coronal and middle curvatures.

An additional consideration when developing models of cyclic fatigue resistance is the canal size. Clinically, different files are more appropriate for different sizes of canals. Therefore, when testing fatigue resistance of a particular file, it is of interest to test the fatigue resistance in different canal sizes. This may provide information on the appropriate file to use depending on the size of the canal being instrumented. In this study, 30/.04 led to a higher NCF compared to 38/.04 and 40/.06, but it also must be considered that Prime files were used in 30/.04 canals and Medium were used in 38/.04 and 40/.06. Therefore, the type of file may have influenced this result. When doing a direct comparison of the mean NCF between Prime and Medium files, Prime files had a significantly higher mean NCF compared to Medium files. However, when all variables were entered into a regression analysis, the type of file did not have a significant influence on NCF. This is likely because the size of the simulated canals were designed to accommodate the sizes of the particular files that would be used in them. One limitation of this

study is that the TruNatomy files were not compared to another file system. TruNatomy's design and size make it a unique file and that is not directly comparable with other file systems on the market. Because of this, different files within the TruNatomy system were compared (Prime and Medium).

An interesting finding with respect to the length of the fractured file fragments is that files in the rotation + axial group tended to have shorted fragment lengths compared to files in the rotation only group. A possible explanation for this is that in the rotation only group each file is rotating in the same spot and so most files (within a particular curvature group) are likely to fracture in a similar location at the maximum point of curvature. With the rotation + axial group, the file is moving axially and the tension and compression forces are distributed along different areas of the files, so it is possible they may not always fracture in the same location and the length could be different compared to the rotation only group.

Temperature was also considered in the current study. A recent study showed that at lower temperatures, these files exhibit greater cyclic fatigue resistance (Shen et al., 2018). If files are being tested at room temperature, for example, the results may not be representative of when they are used on an actual patient. It is important in future studies to keep the temperature of the simulated canals as close to body temperature as possible to be more representative of a clinical scenario.

To achieve the highest possible cyclic fatigue resistance, a file would have to have an A_s an A_f above the average intracanal temperature of 35+/-1°C (Hemptinne et al., 2015). If the A_f value is between room temperature and the intracanal temperature, the file will have a phase transformation, shifting toward a more austenitic phase. This can result in decreased cyclic fatigue resistance (Shen et al., 2013). In the current study, the A_f temperatures for the apical and

coronal segments were 30.32°C and 30.88°C, respectively. For apical and coronal segments, the A_f temperatures were between room temperature and intracanal temperature, indicating that when placed in a canal they may exhibit a phase transformation toward a more austenitic state. This may increase the cutting efficiency, but may lead to a decrease in cyclic fatigue resistance.

Chapter 5: Conclusion

In conclusion, TruNatomy files tested with rotational and axial movement at body temperature exhibited greater fatigue resistance compared to rotational movement alone. It is important that future studies of cyclic fatigue resistance use a model that incorporates both of these movements at body temperature, as it more closely resembles a clinical scenario. Since Prime files had a higher NCF than Medium files, it is important to properly select the file for a particular canal. File tested in apical curvatures exhibited greater fatigue resistance than files tested in curvatures in the coronal and middle third. Therefore, it is important that even when using a very flexible and fatigue resistant file, a proper glide path is developed and a suitable file size is selected when navigating these more coronal curvatures.

Bibliography

Alghamdi S, Huang X, Haapasalo M, et al. Effect of curvature location on fatigue resistance of five nickel-titanium files determined at body temperature. Journal of Endodontics 2020; 46:1682-88.

Bardsley S, Peters CI, Peters OA. The effect of three rotational speed settings on torque and apical force with vortex rotary instruments in vitro. J Endod 2011; 37: 860-4.

Bergenholtz G. Micro-organisms from necrotic pulp of traumatized teeth. Odontologisk Revy 1974;25:347-58.

Brantley WA, Svec TA, Iijima M, Powers JM, Grentzer TH. Differential scanning calorimetric studies of nickel titanium rotary endodontic instruments. Journal of Endodontics 2002;28:567-72.

Cheung GSP. Instrument fracture: Mechanisms, removal of fragments, and clinical outcomes. Endodontic Topics 2009;16:1-26.

Cheung GSP, Bian Z, Shen Y, Peng B, Darvell BW. Comparison of defects in ProTaper hand-operated and engine-driven instruments after clinical use. International Endodontic Journal 2007;40:169-78.

Crump MC, Natkin E. Relationship of broken root canal instruments to endodontic case prognosis: A clinical investigation. Journal of the American Dental Association 1970;80:1341-47.

De Deus G, Moreira EJL, Lopes HP, Elias CN. Extended cyclic fatigue life of F2 ProTaper instruments used in reciprocating movement. International Endodontic Journal 2010;43:1063-68.

De-Deus, G, Vieira VTL, Nogueira da Silva EJ et al. Bending resistance and dynamic and static cyclic fatigue life of Reciproc and WaveOne large instruments. Journal of Endodontics 2014;40:575-79.

Gambarini G, Grande NM, Plotino G, et al. Fatigue resistance of engine-driven rotary nickel-titanium instruments produced by new manufacturing methods. Journal of Endodontics 2008;34:1003-5.

Gao Y, Gutmann JL, Wilkinson K, Maxwell R, Ammon D. Evaluation of the impact of raw materials on the fatigue and mechanical properties of ProFile vortex rotary instruments. Journal of Endodontics 2012;38:398-401.

Gutmann JL, Gao Y. Alteration in the inherent metallic and surface properties of nickel-titanium root canal instruments to enhance performance, durability and safety: A focused review. International Endodontic Journal 2012;45:113-28.

Haapasalo M, Shen Y. Evolution of nickel-titanium instruments: From past to future. Endodontic Topics 2013;29:3-17.

Hemptinne FD, Slaus G, Vandendael M, Jacquet W, De Moor RJ, Bottenberg P. In vivo intracanal temperature evolution during endodontic treatment after the injection of room temperature or preheated sodium hypochorite. Journal of Endodontics 2015;41,1112-15.

Kakehashi S, Stanley HR, Fitzgerald RJ. The effects of surgical exposures of dental pulps in germ-free and conventional laboratory rats. Oral Surgery Oral Medicine Oral Pathology 1965;20:340-49.

Keskin C, Inan U, Demiral M. Effect of interrupted motion on the cyclic fatigue resistance of reciprocating nickel–titanium instruments. International Endodontic Jornal 2018;51:549-55.

Kitchens GG, Liewehr FR, Moon PC. The effect of operational speed on the fracture of nickel-titanium rotary instruments. Journal of Endodontics 2007;33:52-54.

Li U, Lee B, Shih C, Lan W, Lin C. Cyclic fatigue of endodontic nickel titanium rotary instruments: Static and dynamic tests. Journal of Endodontics 2002;28:448-51.

Lopes HP, LD, Elias CN, PhD, Vieira MVB, MSc, et al. Fatigue life of Reciproc and MTwo instruments subjected to Static and dynamic tests. Journal of Endodontics 2013;39:693-96.

Ørstavik, D., & Pitt Ford, T. Essential endodontology: Prevention and treatment of apical periodontitis (2nd ed.) 2008. Blackwell Munksgaard.

Otsuka K, Ren X. Physical metallurgy of Ti-Ni-based shape memory alloys. Progress in Materials Science 2005;50:511-678.

Özyürek T, Uslu G, İnan U. A comparison of the cyclic fatigue resistance of used and new glide path files. Journal of Endodontics 2016;43:477-80.

Panitvisai P, Parunnit P. Impact of a retained instrument on treatment outcome: A systematic review and meta-analysis. Journal of Endodontics 2010;36:775-80.

Peters OA, Arias A, Choi A. Mechanical properties of a novel nickel-titanium root canal instrument: Stationary and dynamic tests. Journal of Endodontics 2020; 46; 994-1001.

Pruett JP, Clement DJ, Carnes DL. Cyclic fatigue testing of nickel-titanium endodontic instruments. Journal of Endodontics 1997;23:77-85.

Ray HA, Trope M. Periapical status of endodontically treated teeth in relation to the technical quality of the root filling and the coronal restoration. International Endodontic Journal 1995;28:12-18.

Ray JJ, Kirkpatrick TC, Rutledge RE. Cyclic fatigue of EndoSequence and K3 rotary files in a dynamic model. Journal of Endodontics 2007;33:1469-72.

Santos LDA, Resende PD, Guiomar M, Bahia DA, Tadeu V, Buono L. Effects of R-phase on mechanical responses of a nickel-titanium endodontic instrument: structural characterization and finite element analysis. The Scientific World Journal 2016;1-11.

Shen Y, Cheung GSP. Methods and models to study nickel-titanium instruments. Endodontic Topics 2013;5:18-41.

Shen Y, Coil JM, Zhou H, Tam E, Zheng Y, Haapasalo M. ProFile vortex instruments after clinical use: A metallurgical properties study. Journal of Endodontics 2012;38:1613-7.

Shen Y, Huang X, Wang Z, Wei X, Haapasalo M. Low environmental temperature influences the fatigue resistance of nickel-titanium files. Journal of Endodontics 2018;44:626-9.

Shen Y, Zhou H, Zheng Y, Peng B, Haapasalo M. Current challenges and concepts of the thermomechanical treatment of nickel-titanium instruments. Journal of Endodontics 2013;39:163-72.

Siqueira JR, Machado AG, Silveira RM, Lopes HP, De Uzeda M. Evaluation of the effectiveness of sodium hypochlorite used with three irrigation methods in the elimination of Enterococcus faecalis from the root canal, in vitro. Journal of Endodontics 1997;30:279-82.

Sobotkiewicz T, Huang X, Haapasalo M, et al. Effect of canal curvature location on the cyclic fatigue resistance of reciprocating files. Clinical Oral Investigations 2021;25:169-77.

Spanberg LSW, Haapasalo M. Rationale and efficacy of root canal medicaments and root filling materials with emphasis on treatment outcome. Endodontic Topics 2002;2:35-58.

Sundqvist G.Bacteriologic studies of necrotic dental pulps. UMEA University Odontological Dissertations 1976;1-93.

Tewari R, Kapoor B, Kumar A, Mishra S, Andrabi S. Fracture of rotary nickel titanium instruments. Journal of Oral Research and Review 2017;9:37.

Topcuoglu HS, Topcuoglu G, Duzgun S. Resistance to cyclic fatigue of PathFile, ScoutRaCe and ProGlider glide path files in an s-shaped canal. International Endodontic Journal 2018; 51:509-14.

Topcuoglu HS, Duzgun S, Akti A, Topcuoglu G. Laboratory comparison of cyclic fatigue resistance of WaveOne Gold, Reciproc and WaveOne files in canals with a double curvature. International Endodontic Journal 2017;50:713-7.

Van der Vyver PJ, Vorster M, Peters OA. Minimally invasive endodontics using a new single-file rotary system. International Dentistry 2019;9:6-20.

Yared G. Canal preparation using only one Ni-Ti rotary instrument: Preliminary observations. International Endodontic Journal 2007;41:339-344.

Walia H, Brantley WA, Gerstein H. An initial investigation of the bending and torsional properties of nitinol root canal files. Journal of Endodontics 1988;14:346-351.